



AEROSERVOELASTICITY INVESTIGATION WITH PANEL METHOD

Ábel OLGAY¹, Béla TAKARICS², Bence KÖRÖSPARTI³, János LELKES⁴, Csaba HORVÁTH⁵, Bálint VANEK⁶

¹ Corresponding Author. Development Engineer, Institute Computer Science and Control. Kende u. 13 - 17, H-1111 Budapest, Hungary. Tel.: +36 1 279 6000, Fax: +36 1 466 7503, E-mail: abel.olgyay@sztaki.hu

² Institute Computer Science and Control. E-mail: takarics@sztaki.hu

³ Institute Computer Science and Control. E-mail: korosparti.bence.balazs@sztaki.hu

⁴ Department of Fluid Mechanics, Faculty of Mechanical Engineering, Budapest University of Technology and Economics. E-mail: lelkes.janos@gpk.bme.hu

⁵ Department of Fluid Mechanics, Faculty of Mechanical Engineering, Budapest University of Technology and Economics. E-mail: horvath@ara.bme.hu

⁶ Institute Computer Science and Control. E-mail: vanek@sztaki.hu

ABSTRACT

When designing a new technological device that is affected by aerodynamic forces, it is almost common practice to model it with 3D CFD methods to study the design and to decide in which direction further developments should be taken. An elastic wing aircraft is considered to be a particularly complex model in which the number of parameters to be tested is too large to consider calculations that take tens or even hundreds of hours per simulation for each factor. In the industry, "high fidelity" Finite Volume Method simulations have become the general practice. Instead we use a so called panel method, where modelling the entire flow field is not necessary, only the surface mesh of the investigated body has to be generated. With this method the computational demand decreases drastically, but we know that there's no such thing as a free lunch. In addition to reducing the calculation time, we need to put the accuracy of the results on the other arm of the balance. The panel method solves only one Laplace equation for the full velocity potential, therefore it cannot model the additional drag due to the viscous medium.

Keywords: Aeroservoelastic Trim, CFD, Elastic wing, Panel Method

NOMENCLATURE

δ_e	[deg]	Elevator deflection
η	[-]	Modal coordinates
Φ	[-]	Mode shape matrix
ρ	$[\frac{kg}{m^3}]$	Density of the fluid
a_i	[deg]	Aileron deflection
C	[-]	Modal damping
C_L	[Pa]	Total pressure
C_M	[m/s]	Absolute velocity vector
$F_{aero,i}$	[N]	Aero force

K	[-]	Modal stiffness
L	[N]	Lift force
M	[-]	Modal mass
M_y	[Nm]	Pitching moment
MAC	[m]	Mean Aerodynamic Chord (MAC)
S	[m ²]	Surface of the wings
T	[-]	Transformation matrix
u	[m]	Displacement
V	$[\frac{m}{s}]$	Free velocity
M_i	[Nm]	Aerodynamic moment

Subscripts and Superscripts

L, D	lift, drag
PS, SS	pressure side, suction side
ref	reference
x, y, z	roll axis, pitch axis, yaw axis

1. INTRODUCTION

The basis of the flight control is a relatively easy task to do if there is only one criteria towards the aircraft: make it fly. But when the originally neglected effects are taken into consideration (such as wind gusts, flutter, drag minimization with aileron deflections), things get more and more complex. In this section a brief overview will be given of the Flipased (Flight Phase Adaptive Aero-Servo-Elastic Aircraft Design Methods) project's aerodynamical development, where an entire investigation model was created for the previously manufactured Flexop UAV. The model was written in Matlab, where the Panukl simulations were controlled with a windows batch file.

2. TRIM CONDITION

The concept of trim condition has to be taken under scrutiny. In this investigation the rate of rota-

tion was neglected, this way a trimmed out aircraft will maintain the set altitude without any rotation around any axes. According to Newton's first law, it leads to the conclusion that the aeroplane will continue in steady rectilinear flight only if the resultant force acting on it is zero, and the resultant moment acting about the center of gravity is also zero. In equations it can be written as:

$$\sum_{i=1}^3 \mathbf{F}_i = 0, \quad (1)$$

$$\sum_{i=1}^3 \mathbf{M}_i = 0, \quad (2)$$

where

- The coordinate axes: $i = \{1, 2, 3\} = \{x, y, z\}$
- The acting forces according to the coordinate axes: \mathbf{F}_i
- The acting momentums according to the coordinate axes: \mathbf{M}_i

It can be written in a dimensionless form. Two dimensionless quantities have to be defined. The lift coefficient and the pitching moment coefficient. (The other two moments around the other two axes are irrelevant in this case due to the symmetrical aircraft geometry, and since the free stream velocity is parallel to the travelling direction.) The describing equations can be seen in equations (3)-(4).

$$C_L = \frac{L}{\frac{1}{2}\rho V^2 S_{ref}} \quad (3)$$

$$C_M = \frac{M_y}{\frac{1}{2}\rho V^2 S_{ref} \cdot MAC} \quad (4)$$

There are important variables in these equations, which have to be described:

- Density of the fluid: $\rho \left[\frac{kg}{m^3} \right]$ (parameter in Panukl).
- Free stream velocity: $V \left[\frac{m}{s} \right]$ (parameter in Panukl).
- Reference area (area of the wings): $S_{ref} [m^2]$ (calculated by Panukl).
- Mean Aerodynamic Cord length: $MAC [m]$ (calculated by Panukl).
- Lift force: $L [N]$ (acts in the z coordinate direction).
- Pitching moment: $M_y [Nm]$ (acts in the y coordinate axis).

To maintain steady rectilinear flight, the lift force and the gravitational force have to be equal, and the pitching moment has to be zero, which means the pitching moment coefficient also has to be zero. The next section is about finding the trim condition in Panukl.

2.1. Finding the trim condition in Panukl

The simulation result, which should be investigated, have to be in trim condition. For this, a modelling method has to be derived. Two variables were taken into consideration when the modelling of the trim condition was derived: the angle of attack and the elevator deflection. Angle of attack (AoA) has the greatest influence in the generated lift force and the elevator flaps are designed directly for pitching moment modification. Two sweeps have been run in Panukl and two variables have been investigated:

Variable sweep

- Angle of attack sweep (0 – 10 [°])
- Elevator deflection sweep (0 – 10 [°])

Investigated variables

- Lift coefficient: $C_L [^\circ]$
- Pitching moment coefficient: $C_M [^\circ]$

When the angle of attack was varied, the elevator deflection was kept at zero and vice versa. The two investigated parameters are plotted below. In Figure 1 the results of the AoA sweep, and in Figure 2 the results of the elevator deflection's results can be seen.

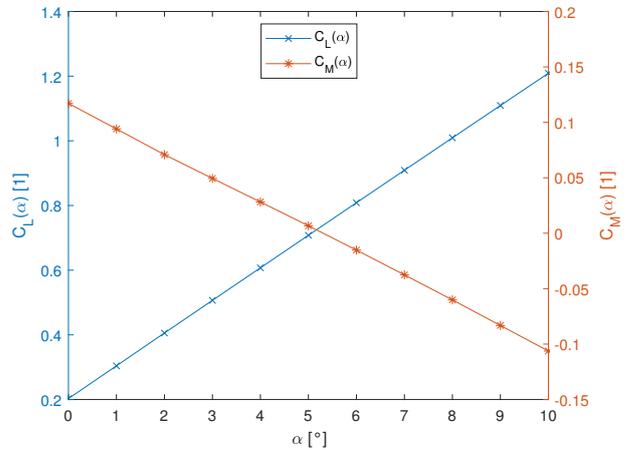


Figure 1. Result of the Angle of attack sweep in Panukl

With a very good approximation, it can be said that the lift coefficient and the pitching moment coefficient are also linear. This property can be seen in the results of the elevator deflection sweep as well.

In the investigated range of angle of attack and elevator deflection, these functions have to be approximately linear. The result of the simulations meets the expectations. Panukl can provide simulation results, which corresponds to those described in the literature [1]. Thus a linear function should be

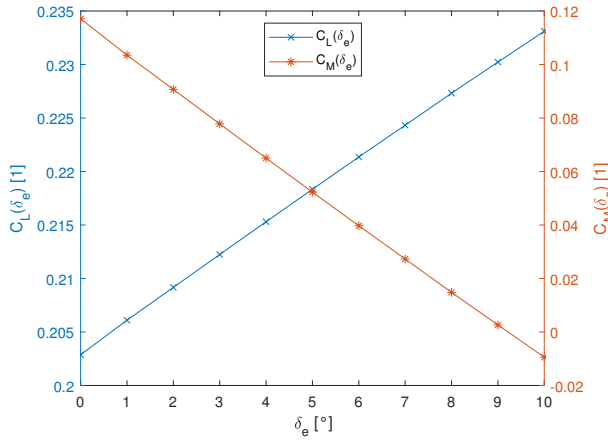


Figure 2. Result of the elevator deflection sweep in Panukl

written in the following form:

$$C_L(\alpha, \delta_e) = C_{L,0} + C_{L,\alpha} \cdot \alpha + C_{L,\delta_e} \cdot \delta_e \quad (5)$$

$$C_M(\alpha, \delta_e) = C_{M,0} + C_{M,\alpha} \cdot \alpha + C_{M,\delta_e} \cdot \delta_e \quad (6)$$

In equations (5)-(6) the constant variables are the following:

$$C_{L,0} = C_L(0, 0)$$

$$C_{L,\alpha} = \frac{\partial C_L(\alpha, \delta_e)}{\partial \alpha}$$

$$C_{L,\delta_e} = \frac{\partial C_L(\alpha, \delta_e)}{\partial \delta_e}$$

$$C_{M,0} = C_M(0, 0)$$

$$C_{M,\alpha} = \frac{\partial C_M(\alpha, \delta_e)}{\partial \alpha}$$

$$C_{M,\delta_e} = \frac{\partial C_M(\alpha, \delta_e)}{\partial \delta_e}$$

Three unknowns require three equations for the coefficients to be sought to be determinable. The set of the simulation parameters can be seen in Table 1.

Table 1. Set of parameters

$(\alpha; \delta_e)$	$C_L(\alpha, \delta_e)$	$C_M(\alpha, \delta_e)$
(0;0)	$C_{L,0}$	$C_{M,0}$
(1;0)	$C_{L,0} + C_{L,\alpha}$	$C_{M,0} + C_{M,\alpha}$
(0;1)	$C_{L,0} + C_{L,\delta_e}$	$C_{M,0} + C_{M,\delta_e}$

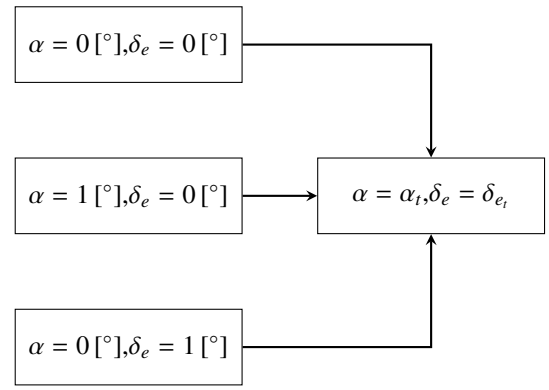


Figure 3. Defining the trim condition

With 3 simulations, the coefficients in the lift and pitching moment functions can be determined, and this way the trim condition can be calculated. As mentioned in section 2, the lift coefficient has to be equal with the non-dimensioning weight of the aircraft and the pitching moment coefficient has to be zero. The AoA and elevator deflection values which correspond to the trim condition are signed with a subscription of "t". All subsequent investigation were performed in trim condition.

2.2. Checking the result

The accuracy of the trim condition modelling can be checked with the help of another run of the simulation using the calculated variables that correspond to the trim condition $(\alpha_t, \delta_{e,t})$. If the investigated coefficients are within an acceptable range of the theoretical value, then the modelling method can be accepted. The results are in Table 2 and Table 3.

Table 2. Simulation parameters

δ_e [°]	8.608
α [°]	-0.270
Ma [1]	0.133

Table 3. Important variables of the simulation

C_l [1]	-1.036e-4
C_m [1]	7.939e-3
C_n [1]	-6.697e-6
C_L [1]	2.088

Two important conclusions can be drawn:

- The pitching moment coefficient is approximately zero, and is close to the other two axis rotation coefficient. The geometry is symmetric to the x-z plane, the side-slip angle was 0°, roll/pitch/yaw rate 0 rad/s, thus these values are caused by numeric error.
- The lift coefficient differs by 0.82% from the theoretical value (0.2105).

With a result like this, it can be said that the modelling method works, and it provides a good approximation for the investigated coefficients.

3. DEFORMATION COMPUTATION

To achieve true trim flight conditions, the elastic deformation of a flexible vehicle may not be ignored, since in this case structural vibration modes

have a larger effect on flight dynamics compared to rigid airframes. To account for this effect, aside from the aerodynamic representation, a structural dynamics model is also required. In this section the methods used in the deformation calculation and their implementation are described.

3.1. Flexible aircraft modeling

To compute the deformation of flexible aircraft, an aerodynamic model, a structural model and an additional method that achieves connection between the two models is used. As previously described, the aerodynamic model computes the aerodynamic load woken on the airframe. A structural representation is created based on the structural properties of the aircraft using the finite element method (FEM). It allows the computation of the deformation due to the aerodynamic load. Since the different models are created using different methods, establishing the connection between them is not a straightforward task. To achieve interconnection of the flexible dynamic system shown in Figure 4., surface spline theory is used, which enables the transformation of aerodynamic forces and moments to the structural model and structural deformation to the aerodynamic model. The result is an iterative process with the undeformed aircraft geometry an structural properties as the input and the deformed geometry as the output.

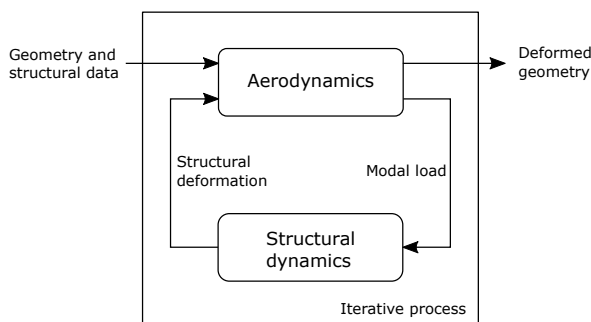


Figure 4. Trim flight deformation calculation process

3.1.1. Structural dynamics model

A brief description of FEM is given here. It is a commonly used modeling tool to perform the analysis of complex structures. Widely employed finite element techniques and procedures are presented in [2] and [3]. Major benefits of this method are its computational efficiency combined with sufficient accuracy of its results.

The linear finite element method separates the geometry into a finite number of beams and nodes with varying structural and geometric properties. The structural model created for the Flipased aircraft has 6 degrees of freedom for each node. The representation can be described in modal coordinates as

$$M\ddot{\eta} + C\dot{\eta} + K\eta = F, \quad (7)$$

where M , C and K represent the modal mass, damping and stiffness matrices respectively, η are the modal coordinates and F is the external excitation expressed in modal coordinates. The matrices are constructed based on the structural properties of the aircraft. The physical displacement u_{struc} of the structural grid expressed in the same coordinate system as the aerodynamic grid can be calculated using the mode shape matrix Φ_{mode} corresponding to the modal coordinates as

$$u_{struc} = \Phi_{mode}\eta. \quad (8)$$

Applying this model allows the computation of the deformed geometry taking the load acting on the aircraft as its input.

3.1.2. Surface spline theory

The surface spline theory is capable of interpolating a given set of deformation using thin plate deformation equations to solve for the unknown deformation at any point on a given surface. This serves as an aid in the transformation of the aerodynamic load to the FEM model and the resulting structural deformation to the aerodynamic grid by adding an in-between step. The spline grid is constructed based on both the structural and aerodynamic grid similarly to the example depicted in Figure 5. The model consists of the structural nodes, each of them complemented by two additional nodes connected to the corresponding central node with a stiff rod. The deformation of the FEM model is transformed as follows: first, all 6 degrees of freedom of the structural grid nodes are transformed purely into heaving motion of the spline grid nodes using the matrix T_{spline} . This allows the structural deformation to be applied on an infinite thin plate and its corresponding equations to be used to interpolate the deformation onto the aerodynamic grid using the matrix T_{plate} . The overall transformation matrix T_{as} used in Equation (10) can be calculated as

$$T_{as} = T_{plate}T_{spline}. \quad (9)$$

$$u_{aero} = T_{as}u_{struc} \quad (10)$$

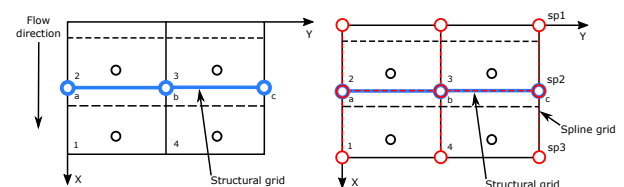


Figure 5. Spline grid

The transformation of the aerodynamic forces and moments require similar steps but in the opposite direction. Firstly, the calculated load components

perpendicular to the thin plate are distributed among the the spline nodes. The resulting load that purely consists of forces is then transformed onto the 6 degrees of freedom of the structural grid. It is important to mention that the effect of the resulting load applied on the structural grid is identical to that of the load applied on the aerodynamic grid. A more detailed description of this process can be found in [4] for which the applied thin plate deformation equations are derived in [5].

3.2. Implementation

The application of the previously described tools begins with the construction of the different models, namely the aerodynamic, the FEM and the spline model. Panukl software is used to model aerodynamics as detailed previously. This representation computes the aerodynamic load acting on the rigid panel model. Pressure coefficients ($C_{p,i}$) are taken from the results to calculate the aerodynamic force (F_i) and moment (M_i) acting on each panel, as in equation (11) and (12).

$$F_{aero,i} = C_{p,i} \frac{\rho}{2} V^2 S_{panel,i} \quad (11)$$

$$\begin{bmatrix} F_i \\ M_i \end{bmatrix} = \begin{bmatrix} 1 \\ \frac{c_{p,i}}{4} \end{bmatrix} F_{aero,i}, \quad (12)$$

where ρ represents air density, V is the airspeed, $S_{panel,i}$ and $c_{p,i}$ are the panel surface and the panel chord corresponding to the i^{th} panel respectively.

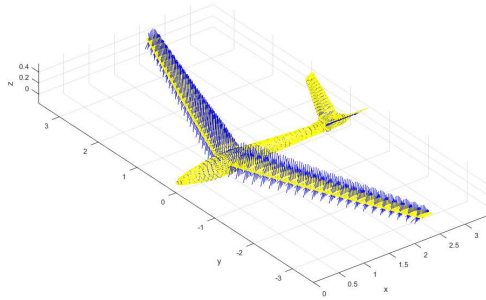


Figure 6. Aerodynamic load calculated from pressure coefficients

These components are applied on the structural grid in the form of modal forces using the surface spline method and the transpose of the mode shape matrix. To convert this load into components that are applicable on the aircraft structure, the spline model has to be built. The spline nodes along the center of every component of the aircraft are geometrically identical to the structural grid points and the outer nodes were created in alignment with these central

nodes based on the aerodynamic model.

The presented spline model is able to account for forces in the z direction and moments acting in the x - y plane. To create a system where the 'x' component of the aerodynamic force is taken into consideration, an additional vertical spline grid can be added to the spline model, which includes the moments acting in the x - z plane as well. The complete spline representation is shown in Figure 7. This additional element promotes a more precise solution for the trim deformation calculation.

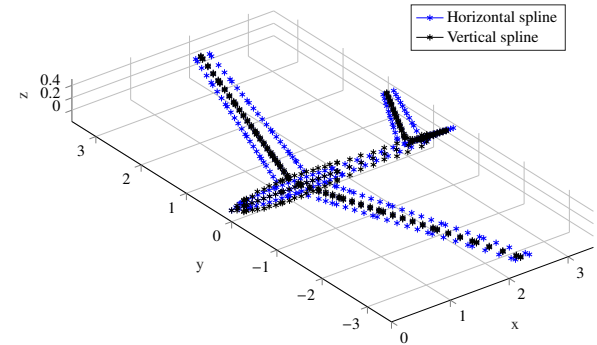


Figure 7. Horizontal and vertical spline

The FEM model is created based on the structural properties of the given airframe. This results in a structural grid for which the dynamic properties are arranged into a state-space model. Here the states are the modal coordinates and their first derivatives. This achieves the solution of Equation (7) with the aerodynamic load expressed in modal coordinates as input and the modal coordinates for the deformed geometry as output.

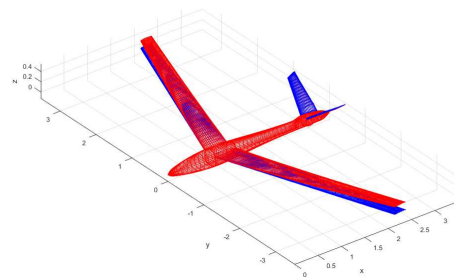


Figure 8. Aerodynamic grid and its deformation

The deformed aerodynamic geometry in Figure 8 will become the input for the next iteration step, where Panukl software takes the leading- and trailing edge coordinates to generate the a new panel model, for which a new set of aerodynamic load will be computed.

4. AEROSERVOELASTIC TRIM CONDITION

All the methods and calculation techniques correspond to a rigid-body aircraft geometry. It is also known that the aerodynamic load deforms the body placed in the flow. This is what happens here as well. The aerodynamic force will bend and twist the aircraft's fuselage, wings, and tails. Due to the change in geometry, the descriptive equations of the aircraft's dynamical behavior will also change. The structural dynamics of the aircraft have been derived by TUM, and the calculations were implemented to Flipased Project by Réka Mocsányi. Only a small description of the derivation was presented earlier. For further information, please refer to [6], [7], [8].

4.1. Finding the aeroservoelastic trim condition

The structural dynamics was implemented into the Matlab model. The geometry deformation was calculated, and the original geometry definition file was rewritten. Nothing was made by hand, everything was handled by a Matlab script. In this way the developed computational method could be implemented in a computational loop. Three simulations are run in every step, in order to calculate the searched trim condition's state variables (α_t, δ_{e_t}), and then another simulation is run with trim conditions. The solution of this simulation is the input of the structural dynamics calculation, the geometry is overwritten based on this, and the loop is moving on to the next step. The calculation loop can be run as long as there is no significant change between two steps of the loop.

First, for research purposes a 10 step long loop was investigated. With the experience of these solutions, a bigger picture can be seen regarding to the importance of these steps. The plots of a few investigated parameters can be seen in Figure 9.

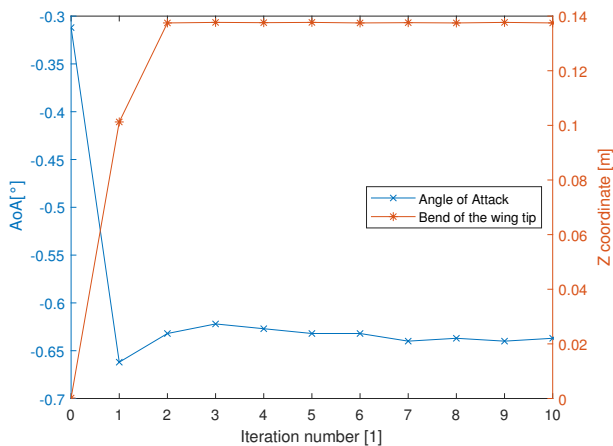


Figure 9. Convergence of some quantities

The 0th iteration number corresponds to the rigid-body simulation. It seems like the elevator deflection converges after just one iteration step, al-

though both the angle of attack and the bending of the wing tip are changing in the further step. With a good approximation 2 iteration steps seem to be enough to reach the converged state, but for a safety reason, for the further calculations 3 iteration steps were set in the modelling method. This converged state is called aeroservoelastic trim condition.

5. RESULTS

5.1. Perturbation around three base values

A simulation investigation has been created, where the perturbation of the aircraft's aileron deflection was investigated. The Flipased UAV has four control surfaces on each wing (symmetrically). Three base angles were chosen ($-2.5 [^\circ]; 0 [^\circ]; 2.5 [^\circ]$), and the perturbation angle was $\pm 0.5 [^\circ]$. This way three sets of simulations were created, where every set contained 81 cases (3^4). One case consisted of a set of aileron deflections, for example $\{a_1; a_2; a_3; a_4\} = \{-2.5; -2.5; -2.5; -2\}$, where a_1 is the closest control surface to the fuselage and a_4 is the farthest. The three sets of simulated base angles resulted in 243 cases. Note that one case means the result of a simulation with aeroservoelastic trim conditions. Thus one result of one case needs 4 simulations in order to attain for the trim simulation, and one rigid body with 3 iterations are calculated in order to find the aeroservoelastic trim condition. Thus the presented example results in 3888 simulations.

The simulations were run on an AMD Ryzen™ 4800H. Panukl can use the CPU cores in parallel mode, but the efficiency is poor. If the simulation ran on only one core, the average occupancy during the simulation was nearly 95%. When Panukl used all the 8 physical cores, this value decreased to 25%. This is due to the poorly optimized parallel calculation in the Panukl solver. In most of the time, the CPU waits for some information. One simulation took approximately 1 minute to finish with the tasks. The Matlab script's run time is negligible (close to 1 second). Thus the 3888 simulations took approximately 2.5 days.

The first presented set of aileron deflections were perturbed around $-2.5 [^\circ]$. The induced drag coefficient was plotted as a function of the wing deflection in Figure 10. Three consecutive values (in the direction of the horizontal axis) belong to the a_4 sweep, where the sweep starts from $-3 [^\circ]$, the second a_4 value is $-2.5 [^\circ]$ and the last one is $-2 [^\circ]$ (from left to right) and every horizontal grid line correspond to a change of one aileron. The grid values can be seen on the bottom of the Figure, where (a_2, a_3) corresponds to the second and third aileron (the smaller the index, the closer it is to the fuselage). One color with a specific marker describes one fixed a_1 value.

In the Figure, it can be seen that the three plots are shifted upwards as the aileron deflection is increased. This means that the first aileron has the biggest effect on the drag force. With a good approx-

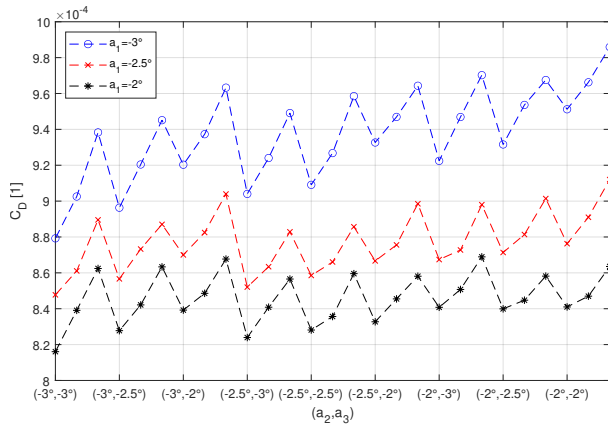


Figure 10. Results of the perturbation (base angle was $-2.5 [^\circ]$)

imation it can be said that the three plotted functions fluctuate around a mean value. There are no peaks or significant increasing/decreasing behavior in the plots.

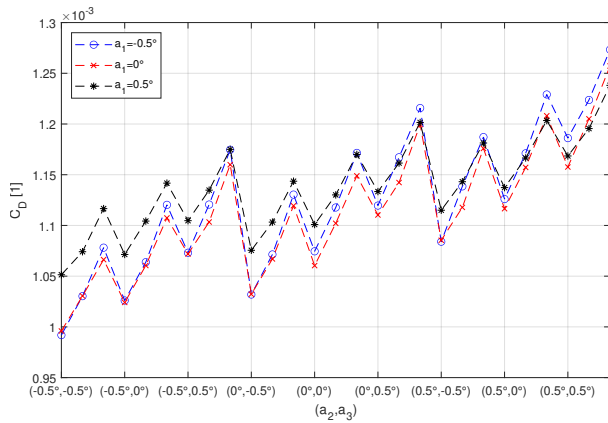


Figure 11. Results of the perturbation (base angle was $0 [^\circ]$)

In both Figure 11 and 12 a constant increasing behavior can be noticed. This kind of trend is caused by the asymmetric aerofoils on the wings. The higher deflection always starts with a higher drag coefficient value, but the slope of the increasing drag coefficient is smaller than the other curves corresponding to other a_1 value. At the bottom-left corner in Figure 11 the highest value belongs to the $a_1 = 0.5 [^\circ]$ case, and the lowest value to the $a_1 = -0.5 [^\circ]$ case, but on the top-right corner they swap places. In Figure 12 this effect is more moderate.

5.2. Effect of different flap deflection angles

Closely similar parameters were investigated as in section 5.1, where the perturbation was investigated. In this section, the perturbation was increased to $\pm 1 [^\circ]$ and the base value was $0 [^\circ]$. The background of the investigation was provided by modern UAV flight control systems. An aircraft's slender wings' structure, as on Flipped UAV, is deformed by

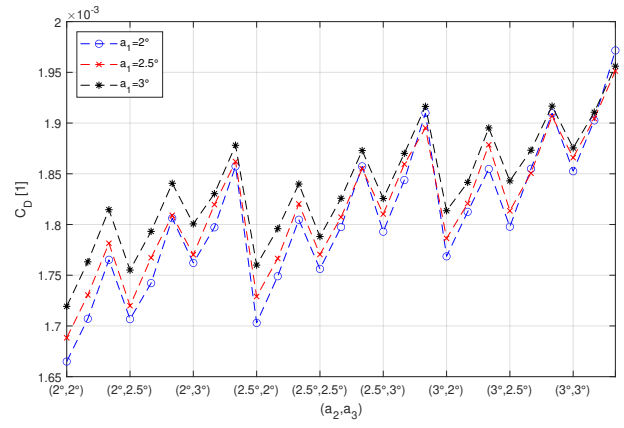


Figure 12. Results of the perturbation (base angle was $2.5 [^\circ]$)

the acting forces on its body, which can cause permanent damage, even wing breakdown. The main acting force is the lift force (more than one magnitude greater than along the other two axes). With ailerons deflected in different directions, most of the lift force generation can be concentrated near to the fuselage, where the lever of the bending motion is small, and the structure is stronger too.

The results of the simulations can be seen in Figure 13. The plot is similar to Figure 11, but this is what can be expected. On one hand, the values are stretched relative to the $\pm 0.5 [^\circ]$ perturbation. The minimal drag is lower, and the highest drag value is greater. A constantly increasing tendency can be noted here too, and the slope of the $a_1 = 1 [^\circ]$ set is smaller than the other two, which change together and are close to each other.

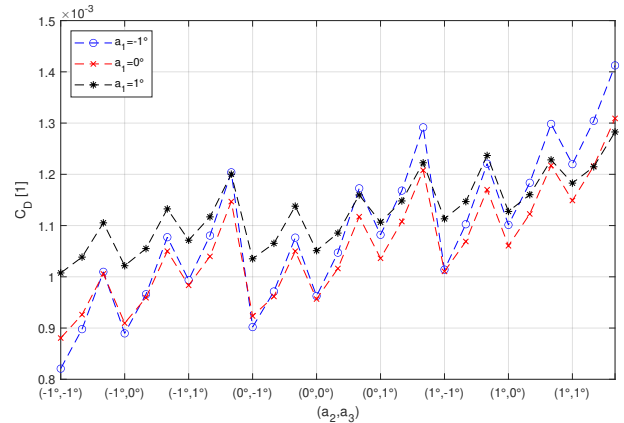


Figure 13. Perturbation with $1 [^\circ]$

5.3. Comparing different solutions

Thiemo Kier from Deutsches Zentrum für Luft- und Raumfahrt (DLR) developed a similar investigation tool-chain, where he used his own aerodynamic solver [9], [10] with Nastran [5]. In DLR, a big data was generated, where the aileron deflection and the velocity has been varied. Later on, an optimization algorithm defined the ideal aileron deflections

for each investigated velocity.

The same velocity and aileron deflection were investigated in Panukl also. The results can be seen in Figure 14. These results correspond to the aeroservoelastic trim condition obtained by two different approaches. The induced drag in Newton dimension can be seen in the vertical axis and the velocity on the horizontal axis. The results approach quadratic functions and it can be concluded, that the two different theoretical approaches show a good match.

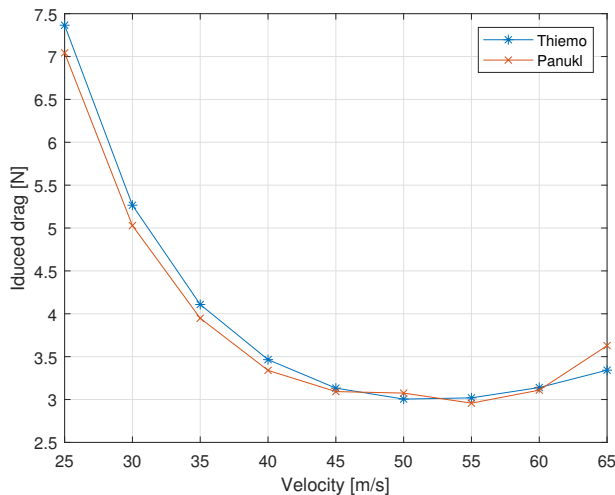


Figure 14. Comparison of the induced drag solutions

6. SUMMARY

A simulation tool-box has been developed and the compared results with different solvers shows good match. In further work, a bigger database will be generated. With the help of these information a control system can be developed, which will take the deformation of the aircraft into consideration, causes lower drag during flight. Lower drag means less burned fuel. With the help of the developed tool-chain, a more environmentally friendly flight condition can be set. If the conclusions can be implemented in bigger aircraft, it could lower the CO₂ emission during a flight.

ACKNOWLEDGEMENT

The research leading to these results is part of the FLiPASED project. This project has received funding from the Horizon 2020 research and innovation programme of the European Union under grant agreement No 815058.

The research was supported by the Ministry of Innovation and Technology NRD Office within the framework of the Autonomous Systems National Laboratory Program.

Supported by the ÚNKP-21-5 New National Excellence Program of the Ministry for Innovation and Technology from the source of the National Research, Development and Innovation Fund.

This paper was supported by the János Bolyai

Research Scholarship of the Hungarian Academy of Sciences.

This project has received funding from the European Union's Horizon 2020 research and innovation programme under grant agreement No 815058.

REFERENCES

- [1] L. Jenkinson, P. Simpkin, D. Rhodes, *Civil Jet Aircraft Design*, 1999, American Institute of Aeronautics and Astronautics
- [2] Klaus-Jürgen Bathe, *Finite Element Procedures*, Book, 2014, Klaus-Jürgen Bathe
- [3] G.R. Liu, *The Finite Element Method: A Practical Course*, Book, 2013, Butterworth-Heinemann
- [4] A. Kotikalpudi, *Robust Flutter Analysis for Aeroservoelastic Systems*, University of Minnesota, Twin Cities, 2017
- [5] William Rodden, *MSC/NASTRAN Aeroelastic Analysis User's Guide*, Book, 1994, MSC
- [6] Wang, Zhicun & Mook, Dean & Gao, David & Hajj, Muhammad R. & Hendricks, Scott & Librescu, Liviu & Preidikman, Sergio. (2004). *Three-Dimensional Configurations, Unstable Aeroelastic Responses, and Control by Neural Network Systems* Zhicun Wang.
- [7] Panda, Chinmaya & S R Pappu, Venkatasubramani. (2009). *Aeroelasticity-In General and Flutter Phenomenon*. 10.1109/ICETET.2009.23.
- [8] T. Luspay, T. Péni and B. Vanek, "Control oriented reduced order modeling of a flexible winged aircraft," 2018 IEEE Aerospace Conference, 2018, pp. 1-9, doi: 10.1109/AERO.2018.8396496.
- [9] Thiemo M. Kier, *An Integrated Modelling Approach for Flight Dynamics, Manoeuvre- and Gust-Loads Analysis*, German Aerospace Center (DLR), 82234 Weßling, Germany
- [10] Thiemo M. Kier, Gertjan H. N. Looye, *Unifying manoeuvre and gust loads analysis models*, German Aerospace Center, Institute of Robotics and Mechatronics, 82234 Wessling, GERMANY